REVIEW ARTICLE
doi: 10.2306/scienceasia1513-1874.2026.008

ScienceAsia 51 (6): 2025: ID 2026008: **1–11**

Near-infrared fluorescent probes for super-resolution imaging

Guoyong Liu[a], **Yen Leng Pak**[b], **Wenxiu Wu**[b], **Yurong Guo**[b], **Zhao Wang**[b], **Yilin Fu**[c], **Yingying Jing**[b,*], **Danying Lin**[d,*]

[a] Shanghai Key Laboratory of Molecular Imaging, Shanghai University of Medicine and Health Sciences, Shanghai 201318 China
[b] College of Biological and Chemical Engineering, Qilu Institute of Technology, Jinan 250200 China
[c] Department of Thoracic Surgery, Shandong Provincial Hospital Affiliated to Shandong First Medical University, Jinan 250021 China
[d] Key Laboratory of Optoelectronic Devices and Systems of Ministry of Education and Guangdong Province, College of Physics and Optoelectronic Engineering, Shenzhen University, Shenzhen 518060 China

*Corresponding authors, e-mail: yyjng@mail.ustc.edu.cn, dylin@szu.edu.cn

Received 22 Aug 2025, Accepted 24 Dec 2025
Available online 15 Jan 2026

ABSTRACT: During the past two decades, super-resolution microscopies (SRMs) have become powerful tools to resolve subcellular structures in a range of 10 nm to 100 nm. Progress in developing fluorescent probes is indispensable for the advancements in SRMs. However, it remains challenging to recognize and observe the bio-complexes in deep imaging depth with high resolution. The emergence of near-infrared (NIR) fluorescent probes brings new light for super-resolution fluorescent imaging due to less light scattering, decreased background signals of auto-fluorescence and low phototoxicity. Thus, in recent years, significant efforts have been made in the development of NIR fluorescence probes for visualizing the fine structures and organizations in cells with high resolution and excellent signal-to-noise ratio. Here we reviewed the recent progress in NIR probes that have been successfully applied to SRMs, including fluorescent proteins, molecular probes, and fluorescent nanomaterials. We also provided a potential prospect on the requirements in future development of NIR fluorescent probes for SRM applications.

KEYWORDS: near-infrared fluorescent probes, super-resolution imaging, biological applications

INTRODUCTION

Unraveling the inner workings of cell activities needs to investigate cells at high resolution. Fluorescence nanoscopy enables relatively safe study of biological phenomena with key advantages of noninvasive labeling, high specificity for targets and high temporal resolution [1–3]. Although various conventional fluorescent imaging tools have been used to investigate vital cellular structures and activities in living bodies, detailed capture of their submicron scale structure cannot be resolved due to the diffraction limitation [4, 5]. In the past two decades, super-resolution techniques offer new visualization possibilities for obtaining sub-diffraction-limit structures at high spatial resolution, leading to a dramatic increase in our knowledge of biomolecule organization and cell function [6]. These super-resolution microscopies (SRMs) are most significantly classed into two different families: (1) one utilizes patterned light to effectively squeeze the diffraction limit, such as stimulated emission depletion microscopy (STED) [7] and structured illumination microscopy (SIM) [8]; (2) another approach achieves super-resolution images based on the localization of single emitting fluorophores, such as (direct) stochastic optical reconstruction microscopy ((d)STORM) [9], photoactivated localization microscopy (PALM) [6], and points accumulation for imaging in nanoscale topography (PAINT) [10]. Now, SRM systems have rapidly expanded as a transformative technology and become popular instruments in the biological and chemical research communities. Several have been developed successfully for deep-tissue and *in vivo* imaging with high spatial resolution [11].

One of the strengths of fluorescence technique is the multiple fluorescent probes which may be applied to label the target. Light with visible wavelengths is largely scattered at great depth, and consequently the penetration of visible light is restricted. The application of present SRMs to living samples or deep tissues are limited owing to shallow imaging depth. Near-infrared (NIR) light can penetrate more deeply into tissues and improve the signal-to-noise ratio (SNR) due to less light scattering in the long-wavelength NIR region [12, 13]. Therefore, NIR fluorescent materials have been exploited to increase the penetration depth of fluorescence signals. Moreover, NIR illumination could diminish the background signals of auto-fluorescence and have low photo damage [14, 15]. Thus, NIR light is ideal for deep tissue imaging especially for super-resolution imaging at great depth with high resolution and better SNR.

NIR fluorescent materials are the cornerstone of NIR super-resolution imaging. Several well-known NIR fluorophores like methylene blue (MB) and indocyanine green (ICG) have been demonstrated for NIR bioimaging with their emissions beyond the visible light region [13]. However, it should be noted that some short emitting dyes performed even better than several fluorophores with long emission beyond

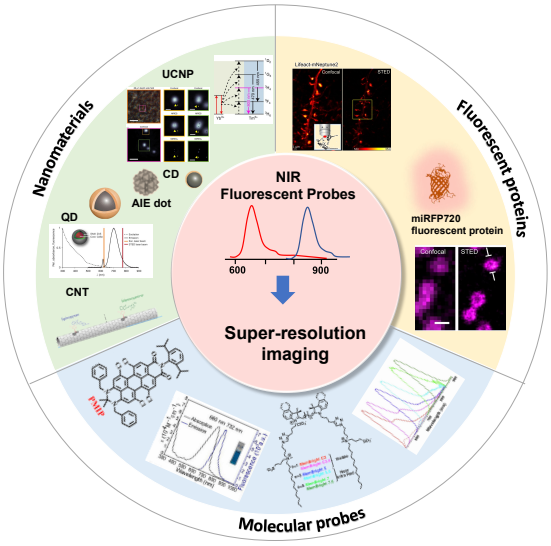

Fig. 1 Schematic illustration of diverse NIR materials used in super-resolution imaging.

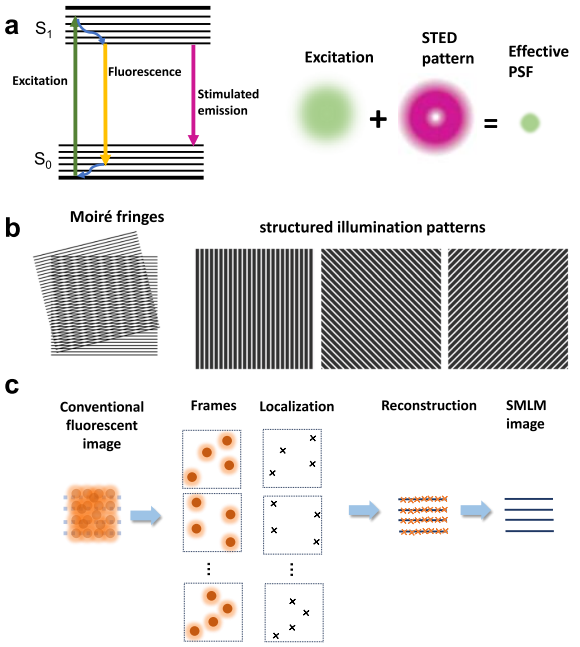

Fig. 2 Schematic of different principles of diverse SRM techniques. (a) Jablonski diagram of fluorescent molecule and the conceptual illustration for STED imaging. The fluorescent emitter is stimulated by an excitation beam. Then the fluorescent is depleted by a doughnut-shaped STED beam to shrink the PSF spot. (b) Principle of SIM technique to image indistinguishable architecture by defined periodical illumination [20]. Figure reprinted with permission from *IOP Publishing*. (c) The ring structures are blurry when all the emitters are excited simultaneously. Single molecule localization (SML) is realized by active control of emission, yielding a sparse record of fluorophores in a single frame. All the localizations are reconstructed into a super-resolved SML image.

1000 nm, which illustrates that wavelength is not the only factor influencing imaging results [13, 16]. Their photophysical properties also impact the performance in the imaging process, such as the quantum yield, anti-photobleaching capability, photostability and more. Furthermore, the complex biological environment and restricted SRM technique conditions require that the fluorophores should be consistent with the instrument and not sensitive to reactive species. Despite immense challenges, NIR fluorescent materials remain attractive for super-resolution bioimaging.

Good reviews on the NIR fluorescent materials have appeared in recent years. Most works focused on the synthesis and modification of NIR fluorescent materials, their applications for *in vivo* imaging, as well as the functions on medical diagnosis [17–19]. Considering that SRMs becoming more important and useable tools for biologists and chemists, great efforts have been made to develop NIR materials for deeper imaging depth and high-performance fluorescent behavior in cells, tissue and animal models with high resolution. In this review, we summarized the latest advancements in NIR materials for super-resolution imaging, including fluorescent proteins (FPs), small molecule dyes and fluorescent nanomaterials, such as upconverting nanoparticles (UCNPs), quantum dots (QDs), nanographene materials, carbon dots (CDs), aggregation-induced emission (AIE) dots and single-wall carbon nanotubes (CNTs). Meanwhile, we also highlighted the applications of NIR materials from the perspective of live-cell, deep-tissue and *in vivo* imaging (Fig. 1).

BASIC PRINCIPLE OF SRMS

In optical microscopy, the light forms a blurry focal spot with restricted size due to diffraction limit (λ/2NA). A dot-like emitter is recorded as a blur point, named the Airy pattern [21]. Thus, traditional imaging techniques excite all these blur points simultaneously, resulting in large overlapping of Airy patterns. Commonly, super-resolution techniques achieve better resolution than the diffraction limit through two ways: (i) methods using patterned illumination to effectively go beyond the diffraction limitation to achieve resolution below 200 nm, and (ii) single localization-based approaches [5].

The first category introduces methods shaping the light pattern to diminish the size of the point spread function (PSF), such as STED and SIM. STED employs a two-beam combination which applies nonlinear optics to sharpen the excitation beam into a refined sub-diffraction-limited excitation volume [22]. The stim-

ulated emission is triggered to suppress the emission of peripheral fluorophores. Then, the PSF is shaped by depleting illumination at the rim of the focus using a doughnut-shaped beam (STED-beam), allowing only the fluorescence at the center of the ring to emit fluorescence with their natural lifetime (Fig. 2a) [23]. The achievable resolution can be expressed as:

$$\Delta r = \frac{\lambda}{2n \sin\alpha \sqrt{1 + I_{\mathrm{STED}}/I_{\mathrm{S}}}}$$

where λ represents the wavelength, n is the refractive index, α is the collection angle of the objective, I_{STED} corresponds to the intensity of STED illumination, and I_{S} is the intensity of saturated stimulated radiation, respectively. When the intensity of the STED-beam is higher, the central area with zero intensity is smaller. Thus, the resolution was enhanced in STED imaging as the intensity of the depletion beam increased [24]. In addition, the saturated stimulated emission intensity is inversely determined by the fluorescence lifetime τ_{fl} of the probe and the absorption cross-section σ of the STED light. Compared to the dispersed molecular dyes, the compact nanomaterials usually have larger optical cross-sections, which conduce to lower saturation intensity or higher depletion efficiency. Moreover, inorganic materials, such as UCNPs and QDs, usually have longer lifetimes, which also cause a low saturation intensity.

Besides the emission depletion pattern, the SIM technique enhances resolution through frequency mixing between a patterned excitation and the sample, introducing low-frequency Moiré fringes that can be resolved by traditional optical microscopy [25]. By acquiring multiple images with illumination patterns of different phases and orientations, a super-resolved picture is finally reconstructed based on a lot of original images using algorithms (Fig. 2b) [20]. The illumination pattern is restricted by the diffraction limit of light, thus, SIM is capable to achieve a resolution of $\sim$ 100 nm in the lateral direction and $\sim$ 300 nm in the axial direction by calculating diffraction-limited original images.

Another category is the accumulation of single-molecule localization of sparse fluorophores, like PALM, STORM and PAINT. These methods accurately determine the centers of individual PSFs, rather than detecting all fluorescent signals simultaneously. The center of a single PSF can be calculated by various methods, such as least-squares fitting, Gaussian fitting and maximum likelihood estimation [9]. By repeating this cycle of activation, localization, and deactivation, the positions of a sufficient number of labeled fluorophores can be determined (Fig. 2c) [4]. Usually, PALM initially used photoactivable fluorescent proteins that can be activated by light with a wavelength different from the excited light. STORM employed photoswitchable dyes for the ON and OFF signal recording. In PAINT method, fluorescence molecule sparse detection based on instantaneous combination and separation of targeted probes and dispersed fluorescent molecules in solution. The reconstructed image from the localizations depends not only on the microscope but also on the fluorescent materials applied to label the targets. The localization density, photons per switching event, and on/off duty cycle (DC) are important to the fluorescent materials, which largely influence the quality of super-resolution images [21].

KEY CONSIDERATIONS FOR FLUORESCENT PROBES UNDER DIFFERENT SRMS

The key to all fluorescent SRMs achieving NIR imaging hinges on the selection of appropriate fluorescent probes. In addition to the need for excitation and emission at NIR wavelengths, each technique has distinct criteria for ideal NIR probes. To enhance bioimaging and biosensing performance, several essential principles must be considered in the development of NIR fluorophores, such as NIR fluorescence brightness, absorption and emission wavelengths, anti-bleaching capability, and photostability [26]. Apart from that, the NIR fluorescent probes also have a higher benchmark for obtaining high resolution in SRMs.

In general, the fluorescent probes for STED demand low saturation intensity and excellent anti-photobleaching capability to enhance the resolution. Thus, the fluorophores are desired to achieve high photostability and resist photobleaching. Recently, the application of inorganic nanocrystal materials as probes is in its infancy in STED imaging, such as UCNPs [27] and QDs [28]. SIM is the closest to conventional fluorescence microscopy, needing no special probes but, due to the fact that multiple intermediate frames are recorded, anti-photobleaching must be taken into account [29]. During single-molecule localization imaging, fluorophores stochastically switch between active and inactive states, and the localization precision relies on the number of photons collected during each on-time of the fluorophore [30]. Efficient labeling density, high localization precision, and a small recognizing footprint are vital for well-defined single-molecule localization images [31].

FLUORESCENT PROTEINS

FPs enable straightforward and specific labeling of targets without the need to deliver any additional substances, making a less significant impact on the organisms [32]. Thus, FPs are indispensable for live-cell imaging and *in vivo* imaging. A key challenge in applying SRMs to *in vivo* imaging is seeking suitable FPs that offer deep tissue penetration, high brightness, and photostability. NIR FPs are especially desirable because they can be fused to protein domains to generate labels for monitoring dynamic behaviors within deep tissues and living animals [33]. However, efforts to design FPs

Table 1 Photophysical properties of several NIR FPs, which are relevant for super-resolution imaging.

FP	λ_{ex} (nm)	λ_{em} (nm)	ε_{abs} (M^{-1} cm^{-1})	Quantum yield	Quaternary structure	Ref.
PSmOrange	636	662	32700	0.28	monomer	[34]
mNeptune2	599	651	89000	0.24	monomer	[35]
E2-Crimson	605	646	126000	0.23	tetramers	[36]
mGarnet	598	670	95000	0.09	monomer	[37]
TagRFP657	611	657	34000	0.10	monomer	[38]
miRFPs720	702	720	96000	0.06	monomer	[39, 40]

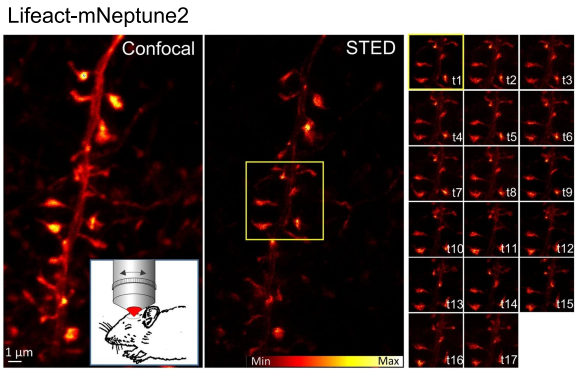

Fig. 3 Representative super-resolution imaging of mNeptune2 FP for *in vivo* STED imaging. Confocal mode with 560 nm excitation and STED mode with an additional laser at 732 nm were used for imaging the dendritic branch at a 6 µm depth of the visual cortex [4]. Figure reprinted with permission from *Springer Nature*.

with maximum excitation exceeding 600 nm usually result in undesired diminishment in brightness [12].

Table 1 lists the photophysical properties of some typical red-emitting and NIR-emitting fluorescent proteins used for imaging in living bodies [34–40]. Pennacchietti and coauthors reported the phenomenon of near-infrared to far-red photoconversion in the miRFP family, which was engineered from bacterial phytochromes. They achieved NIR STED imaging and followed the dynamics of lysosomes tagged with miRFP720 in live U2OS cells with higher resolution than conventional microscopy [39]. Additionally, Wegner and co-workers applied mNeptune2 FP in STED imaging in vivo. They realized super-resolution visualization of the F-actin structure at 6 µm depth of the visual cortex (L5 to L1) in a living mouse for time periods of up to 1 h (Fig. 3) [41]. With the development of advanced mutagenesis and screening strategies, more enhanced NIR FPs or even entirely novel NIR FPs will be applied to obtain more valuable information for NIR super-resolution imaging.

MOLECULAR PROBES

Generally, FPs are biocompatible and exhibit low cytotoxicity. However, the low photon count might lead to lower localization precision. Comparatively, organic dyes, which can be tuned to desirable emission colors by adjusting their structures, are regarded as potential candidates for biological imaging [42]. Although several NIR dyes could act as photosensitizers to generate reactive oxygen species (ROS) to participate in photodynamic therapy, those dyes usually have low toxicity under the imaging concentration [43–45]. Compared with the potential toxicity caused by heavy metal elements in inorganic materials, small-molecule NIR dyes are particularly appealing for fluorescent imaging due to their high design flexibility, small size and high biocompatibility. Various NIR fluorophores with defined small-sized structures have been exploited and employed in SRMs, e.g., cyanine, BODIPY, xanthene, and squaraine [45–47].

For example, cyanine-based fluorophores such as Cy3 and Cy5 are widely used in STORM [50]. Collot et al [48] developed a series of membrane-targeted dyes named MemBright. The family of MemBright fluorescent molecules can recognize the cell membrane efficiently and are compatible with long-term fluorescent imaging within tissues and live cells (Fig. 4a). In addition, the oxygen position of the xanthene core could be substituted for different heteroatoms such as Si, emitting NIR fluorescence with high photostability [51, 52], such as Yale676sb, which was synthesized to emit in the NIR region and has a high quantum yield of 0.59 [53]. Besides, in 2024, a novel small chromophore PMIP, which has an emission maximum at 732 nm, was developed to realize the single-molecule imaging of lysosomes [54]. Salam et al [49] presented a highly photostable NIR-emitting Zn-complex structure for the dynamical distribution and long-time tracking of lysosomes in *Caenorhabditis elegans* (Fig. 4b). A smallest-size lysosome ($\sim$ 77 nm) was captured by the zinc metal complex *in vivo* during embryogenic evolution.

Moreover, several research groups have integrated genetically encoded methods with organic dyes for achieving super-resolution imaging *in vivo*. Initially, the targeted protein is fused with tags, such as Halo or SNAP tag [56]. These tags then covalently bind to their corresponding fluorescent dyes. More significantly, these tags are combined with NIR dyes for *in vivo* imaging. For example, the Stefan W. Hell group took advantage of the NIR SiR combining with Halo tag to realize STED super-resolution *in vivo* imaging of postsynaptic density protein-95, achieving outstanding

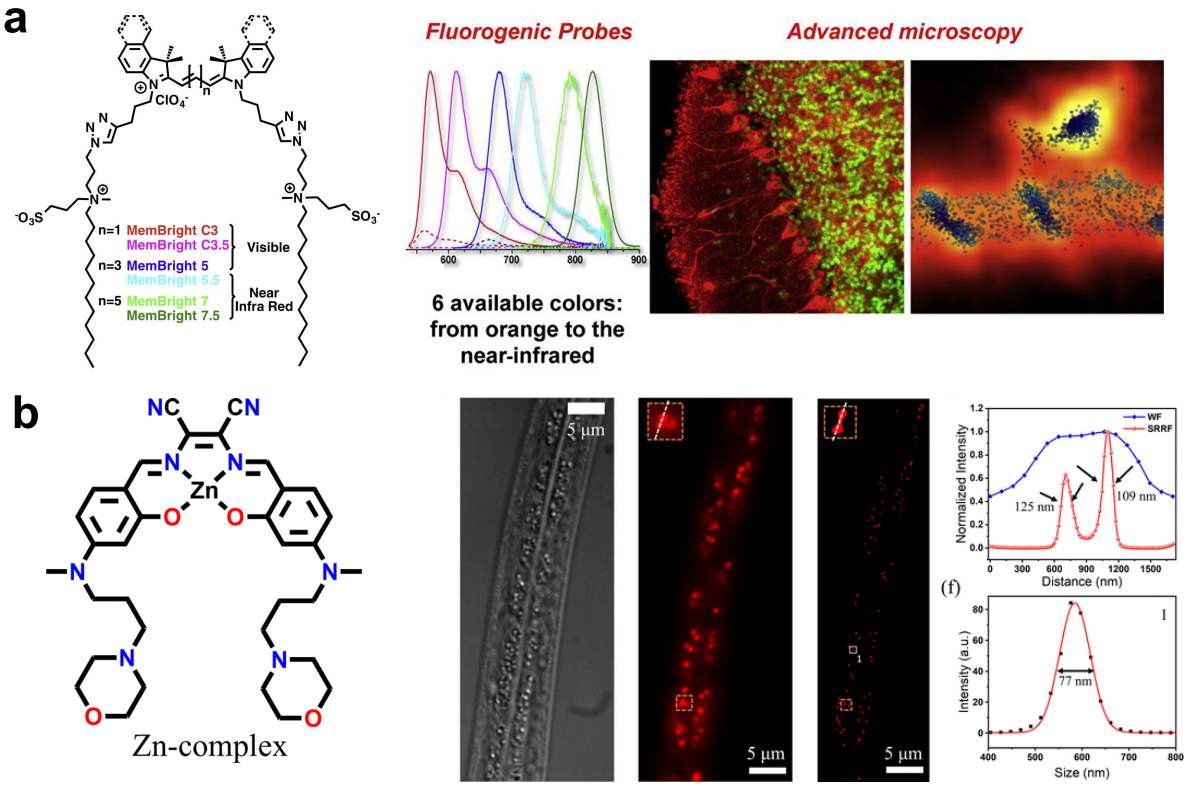

Fig. 4 Structure and applications of molecular NIR dyes for super-resolution imaging. (a) Structure and emission spectra of different MemBright probes. These diverse dyes were utilized for staining membranes within live cells and tissues [48]. Figure reprinted with permission from *Elsevier*. (b) Structure of the Zn-complex and applications of the Zn-complex to image the lysosomes throughout the whole *C. elegans* [49]. Figure reprinted with permission from *Royal Society of Chemistry*.

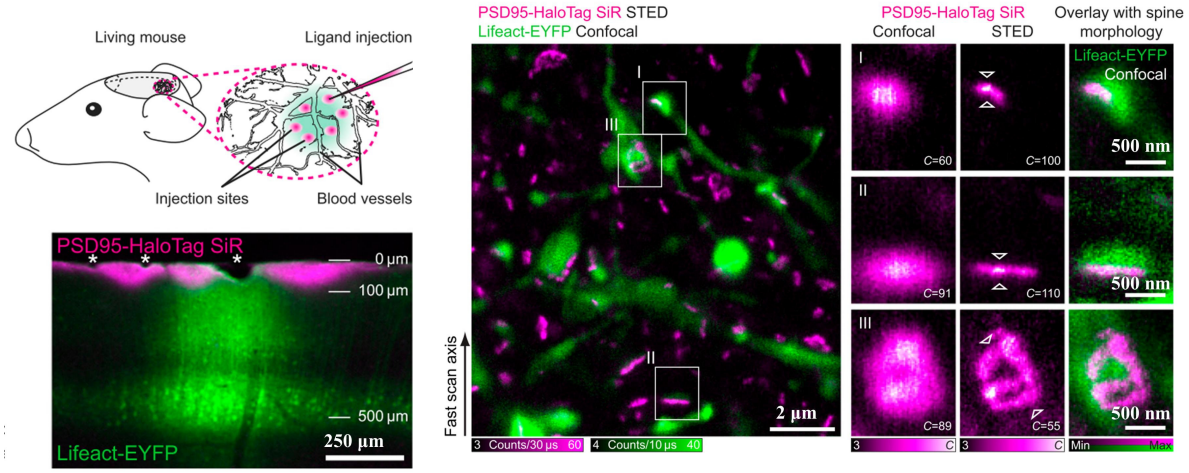

Fig. 5 Schematic illustration of the injections of SiR-Halo at multiple sites in the region of EYFP reference expression. The Lifeact-EYFP-expressing pyramidal neurons are located at a depth of ∼ 500 µm below the cortical surface. The SiR-Halo labeling extended down to 100 µm. The STED images show the PSD95 scaffolds *in vivo* [55]. Figure reprinted with permission from *National Academy of Sciences USA*.

fluorescence contrast and photostability. Compared with FPs, NIR SiR enabled z-stack acquisition and repeated imaging at STED resolution [55]. They found that PSD95 formed diverse nanoscale organization patterns with large variations in size and shape among individual synapses (Fig. 5). As organic dyes continue to improve, the application of NIR organic dyes in SRMs is becoming increasingly viable. However, ongoing efforts are still needed to further enhance NIR dyes for future SRMs studies in living animals.

FLUORESCENT NANOMATERIALS

Fluorescent nanomaterials, such as UCNPs, QDs, CDs, AIE dots and CNTs, have attracted great attention in super-resolution imaging due to their excellent photophysical characteristics [57, 58]. The photostability of nanomaterials is commonly superior to that of organic dyes, and they have promising properties achieved by adjusting their structures and modifying components [59, 60].

UCNPs are a kind of fluorescent materials that provide a saturation intensity two orders of magnitude lower than that of small-molecule dyes. UCNPs convert the long NIR excitation (750–1,000 nm) to short ultraviolet (UV) and visible emission, attracting large attention of researchers in the past decade. Chen et al [61] reported a near-infrared emission saturation (NIRES) microscopy, employing UCNPs for super-resolved visualization at deep imaging depth. The excitation intensity was several orders of magnitude smaller than that demanded by organic molecules. They achieve a resolution of sub 50 nm by using a doughnut beam excitation from a 980 nm diode laser and detecting at 800 nm. Fig. 6a shows a bright-field image of an 88 µm liver tissue slice using 4% Tm^{3+}, 40% Yb^{3+} co-doped UCNPs with excitation power density of 5.5 MW/cm^2 [61]. Moreover, in 2020, Liu et al [62] proposed an upconversion nonlinear SIM (U-NSIM) approach using ytterbium (Yb^{3+}) and thulium (Tm^{3+}) co-doped UCNPs. They achieved a resolution below 131 nm through Wiener deconvolution (top) and U-LSIM (Fig. 6b).

QDs exhibit higher photostability and brightness than organic dyes, making them promising alternatives for fluorescent imaging [66]. QDs typically have a narrow emission region and can be freely tuned throughout the entire visible spectrum [67]. Moreover, they are commercially available and can be modified to be live-cell compatible by coating with standard coupling chemistry [68]. Hanne et al [63] applied a kind of QDs, which named as Qdot705, for STED imaging with an excitation wavelength of 628 nm and a STED wavelength of 775 nm (Fig. 7a). This enabled enhanced resolution for imaging single QDs and vimentin fibers in cells.

By adjusting the precursor and reaction conditions, CDs can realize excellent photostability, photoblinking, and photofluctuation properties [69]. Thus, CDs have drawn large attention as promising materials for SRMs. In 2025, Liu et al [70] demonstrated that polarization facilitated the surface state emission of CDs through a single decay pathway, while hydrogen bonding was identified as a factor that hindered the surface state emission of CDs through non-radiative decay. They applied the yellow-emitting CDs in dual-color super-resolution fluorescence imaging in living cells. Graphene quantum dots (GQDs) are nanoscale graphene fragments with well-defined, quantized energy levels and have recently been proposed as an environmentally friendly alternative to CDs and QDs [71]. In recent works, nanographene materials with nanoscale graphene structures presented superior properties [57]. Fang et al [64] developed a NIR lysosome-targeted imaging nanoaggregate HD-Br based on the hemicyanine structure. They applied the HD-Br nanoaggregates for 3D imaging of lysosomes in live *C. elegans* (Fig. 7b).

AIE refers to a weakly emitting or non-emissive fluorescence phenomenon in solution, however, they turn into strongly fluorescent state in solid form [72]. AIE has caught large interest in exploiting new fluorescence probes for SRMs. The organic dots with AIE characteristics have emerged as powerful tools owing to their high brightness, high photostability, and low toxicity. Recently, many exciting works reported that properly designed AIE dots can reach the NIR-emission region, and also have great potentials in super-resolution imaging. For example, Xu et al [65] developed an AIE nanocrystal in the deep-red region named DTPA-BT-F, which has photoluminescence quantum yield (PLQY) of 36.49%. The probe could capture lysosomes in cells and achieve superior resolutions under a much lower STED power as shown in Fig. 7c.

CNTs are remarkable nanostructures that have garnered extensive attention in the imaging community due to their strong optical resonances in the NIR region. In 2019, Godin et al [73] reported the design and imaging implementation of photoswitchable CNTs, which had controlled blinking behaviors at the single-nanotube level in the near infrared region. Fig. 8 illustrates two segments that could be separated about 320 nm apart from each other, which is hard to achieve with the conventional far-field image [73].

Despite the fact that a series of fluorescent nanomaterials have been extensively employed for SRMs, none of those nanomaterials are ideal or without shortcomings. For instance, the applicability of QDs in SRM is restricted by their fast blinking and toxicity. Table 2 listed the main characteristics of representative fluorescent materials for diverse SRMs. Moreover, the advantages and disadvantages also compared for better selection of suitable probes for bio-imaging. Therefore, exploring for an appropriate extrinsic NIR nanomaterial for SRMs is thus ongoing.

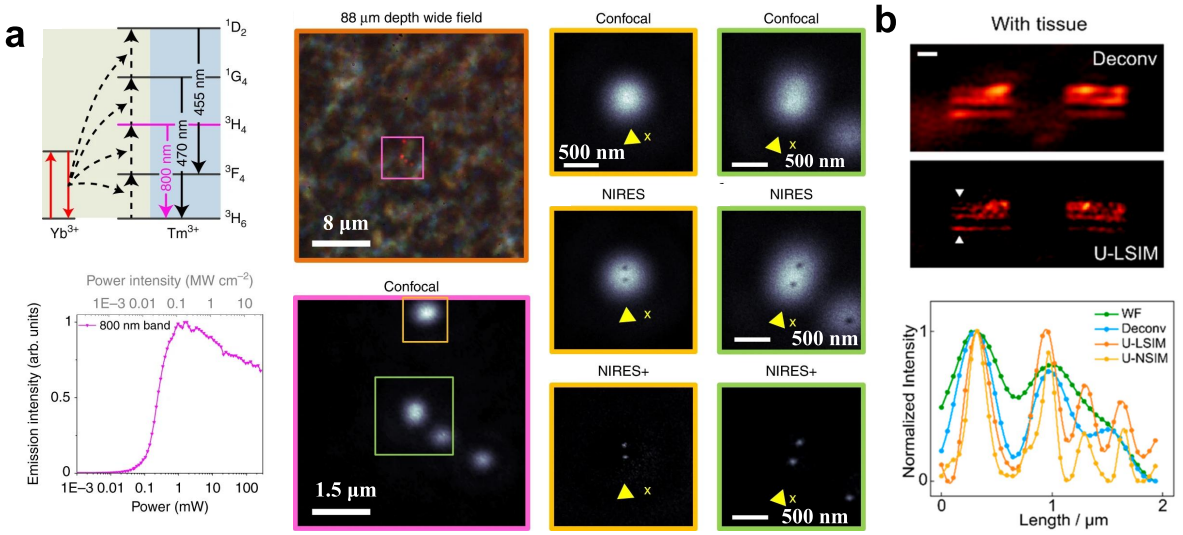

Fig. 6 Applications of UCNP nanomaterials for SRMs. (a) The upconversion process of Tm^{3+} and Yb^{3+} co-doped UCNPs, and the emission intensity curve from UCNPs (40 nm $NaYF_4$: 20% Yb^{3+}, 4% Tm^{3+}) under 980 nm excitation. The developed UCNPs were utilized for STED imaging at 88 μm depth in a mouse liver tissue slice [61]. Figure reprinted with permission from *Springer Nature*. (b) Left: Wiener deconvolution (top) and upconversion nonlinear SIM U-LSIM (bottom) of a 51.5 μm liver tissue slice. Right: the normalized intensity of the cross-section profile under different conditions in the left image [62]. Figure reprinted with permission from *American Chemical Society*.

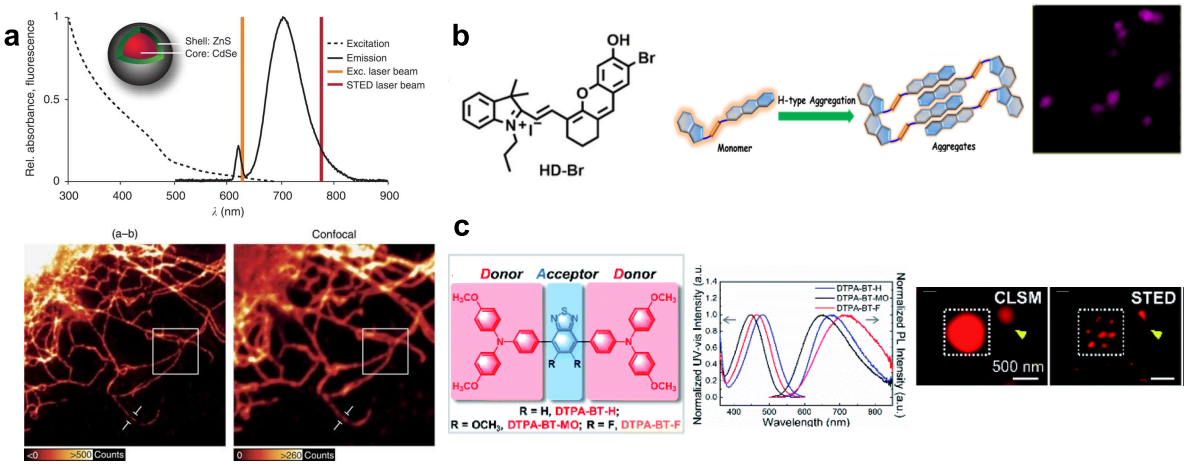

Fig. 7 Examples of QDs, CDs and AIE dots for super-resolution imaging. (a) STED imaging of cellular vimentin fibers using Qdot705 [63]. Figure reprinted with permission from *Springer Nature*. (b) Structure of HD-Br and the H aggregation of HD-Br in aqueous solution. The SIM image shows *C. elegans* labeled with the developed HD-Br Nanoaggregates [64]. Figure reprinted with permission from *American Chemical Society*. (c) An AIE nanocrystal with deep-red emission for STED super-resolution imaging [65]. Figure reprinted with permission from *Royal Society of Chemistry*.

CONCLUSION AND OUTLOOK

In conclusion, we provided a short review of the recently developed NIR fluorophores for super resolution imaging. We first described the basic principles of different super-resolution techniques and emphasized the key considerations for fluorophores in diverse SRMs. Subsequently, we discussed the current NIR FPs, small-molecule dyes and nanomaterials for the applications in SRMs. Even though considerable efforts have been expended toward developing NIR fluorescent probes for *in vivo* imaging, high-performance fluorophores for super resolution imaging are still limited in achieving high resolution and deep imaging depth.

Super-resolution fluorescence imaging is always a trade-off among the acquisition speed, spatial res-

Table 2 Summary of representative fluorescent materials for super-resolution imaging.

Category	Size	Techniques	Applications	Advantages	Disadvantages	Ref.
FPs	<1 nm	STED; SIM; PALM	Observing morphological changes of actin in the cortex of a living mouse;	High biocompatibility	Low brightness	[25, 37, 41]
Molecular probes	<1 nm	STED; SIM; STORM	Imaging proteins and organelle sand in live cells	Structure adjustable	Potential toxicity	[15, 46, 51, 53, 54]
UCNPs	10∼30 nm	STED; SIM	Deep tissue imaging	Sharp emission band	Poor water solubility	[27, 61, 62]
QDs	10∼20 nm	STED; SIM; STORM	Cellular and subcellular structure imaging; real-time tracking	Tunable particle size and surface modification	Potential toxicity of heavy metals	[63, 67, 74]
CDs	2∼7 nm	STED; SIM; STORM	Deep tissue imaging	Water-soluble and biocompatible	Rare red and infrared emission	[70, 75, 76]
AIE dots	10∼50 nm	STED	Cellular and subcellular structure imaging	Tunable surface functionality	Limited choice	[65, 72]
CNTs	0.4∼10 nm in diameter; 100 nm ∼ 1 µm in lengths	STORM	individual CNTs	Emission in NIR-I and NIRII windows	Poor water solubility	[73, 77]

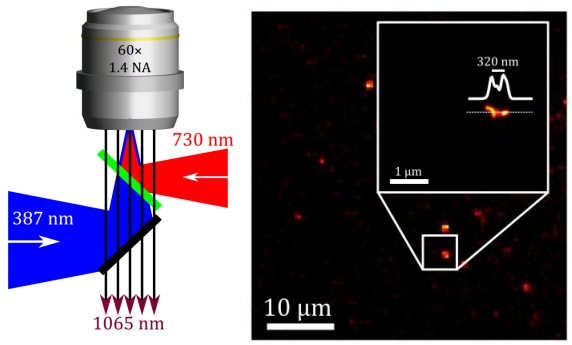

Fig. 8 Schema showing the fluorescence setup for CNTs imaging with UV illumination. Super-resolved images display different nanotube segments about 320 nm apart [73]. Figure reprinted with permission from *American Association for the Advancement of Science*.

olution, and compatibility with the biological system. Rapidly progressing towards NIR probes has promoted victories on applications of SRMs *in vivo* and deep tissue. Nevertheless, there are some limitations remain to be overcome in the future progression and application of NIR probes for super-resolution imaging. First, high-performance NIR fluorescent materials should be bright enough with targets. Due to the complex network biological environment, only probe with sufficient brightness can lead to more accurately positioning. The high brightness of nanomaterial provided large options to allow functional portions to be designed for a given application. Second, longer emission wavelengths of fluorophore are still lacking. For instance, few dyes with emissions exceeding 1200 nm are available, which limits further imaging *in vivo*. Last but not least, more strategies are desired for the development of specific biosensing probes. Thus, future efforts could be made to develop specific probes that can respond to targets and have differentiable signals for various analytes.

Of course, efforts in the construction of optical systems, camera technologies and labeling strategies should make progress together to make it possible to view multiple cellular structures and biological activities in living species with high resolution. We anticipate that this minireview will assist researchers in comprehensively grasping the developing trends underlying NIR fluorophores for enhanced super-resolution imaging.

Acknowledgements: This work was supported by the Natural Science Foundation of Shandong Province (ZR2024QC200 and ZR2022QB218), the construction project of Shanghai Key Laboratory of Molecular Imaging (18DZ2260400), the National Natural Science Foundation of China (62235007 and 62275165), and the Taishan Scholar Young Talent Program (tsqn202211249).

REFERENCES

1. Carsten A, Wolters M, Aepfelbacher M (2023) Super-resolution fluorescence microscopy for investigating bacterial cell biology. *Mol Microbiol* **121**, 646–658.
2. Qu J, Luo G, Li S, Qi K, Hu R, Li J, Liu L, Chen Y, et al (2024) Label-free *in vivo* monitoring of lipid droplets for real-time assessment of adipose activator-induced tumor suppression. *Anal Chem* **96**, 2754–2758.
3. Mo L, Wang X, Liu X, Gao J, Tan C, Jian S (2024) Role and mechanism of FDFT1 in regulating ferroptosis in colon cancer cells via the Nrf2/GPX4 pathway. *ScienceAsia* **50**, ID 2024038.

4. Mockl L, Moerner WE (2020) Super-resolution microscopy with single molecules in biology and beyond-essentials, current trends, and future challenges. *J Am Chem Soc* **142**, 17828–17844.
5. Schermelleh L, Ferrand A, Huser T, Eggeling C, Sauer M, Biehlmaier O, Drummen GPC (2019) Super-resolution microscopy demystified. *Nat Cell Biol* **21**, 72–84.
6. Baddeley D, Bewersdorf J (2018) Biological insight from super-resolution microscopy: What we can learn from localization-based images. *Annu Rev Biochem* **87**, 965–989.
7. Vicidomini G, Bianchini P, Diaspro A (2018) STED super-resolved microscopy. *Nat Methods* **15**, 173–182.
8. Li Z, Zhang Q, Chou S, Newman Z, Turcotte R, Natan R, Dai Q, Isacoff EY, et al (2020) Fast widefield imaging of neuronal structure and function with optical sectioning *in vivo*. *Sci Adv* **6**, eaaz3870.
9. Liu H, Ye Z, Deng Y, Yuan J, Wei L, Xiao L (2023) Blinking fluorescent probes for single-molecule localization-based super-resolution imaging. *Trends Anal Chem* **169**, 117359.
10. Reinhardt SCM, Masullo LA, Baudrexel I, Steen PR, Kowalewski R, Eklund AS, Strauss S, Unterauer EM, et al (2023) Ångström-resolution fluorescence microscopy. *Nature* **617**, 711–716.
11. Jing Y, Zhang C, Yu B, Lin D, Qu J (2021) Super-resolution microscopy: Shedding new light on *in vivo* imaging. *Front Chem* **9**, 746900.
12. Reja SI, Minoshima M, Hori Y, Kikuchi K (2021) Near-infrared fluorescent probes: A next-generation tool for protein-labeling applications. *Chem Sci* **12**, 3437–3447.
13. Lei Z, Zhang F (2020) Molecular engineering of NIR-II fluorophores for improved biomedical detection. *Angew Chem Int Ed* **60**, 16294.
14. Zhao J, Ma T, Chang B, Fang J (2022) Recent progress on NIR fluorescent probes for enzymes. *Molecules* **27**, 5922.
15. Lukinavicius G, Umezawa K, Olivier N, Honigmann A, Yang G, Plass T, Mueller V, Reymond L, et al (2013) A near-infrared fluorophore for live-cell super-resolution microscopy of cellular proteins. *Nat Chem* **5**, 132–139.
16. Li L, Dong X, Li J, Wei J (2020) A short review on NIR-II organic small molecule dyes. *Dyes Pigments* **183**, 108756.
17. Tiwari DK, Tiwari M, Jin T (2020) Near-infrared fluorescent protein and bioluminescence-based probes for high-resolution *in vivo* optical imaging. *Mater Adv* **1**, 967–987.
18. Huang J, Pu K (2021) Near-infrared fluorescent molecular probes for imaging and diagnosis of nephro-urological diseases. *Chem Sci* **12**, 3379–3392.
19. Yang F, Zhang Q, Huang S, Ma D (2020) Recent advances of near infrared inorganic fluorescent probes for biomedical applications. *J Mater Chem B* **8**, 7856–7879.
20. Sezgin E (2017) Super-resolution optical microscopy for studying membrane structure and dynamics. *J Phys Condens Matter* **29**, 273001.
21. Biteen J, Willets KA (2017) Introduction: Super-resolution and single-molecule imaging. *Chem Rev* **117**, 7241–7243.
22. Kamper M, Ta H, Jensen NA, Hell SW, Jakobs S (2018) Near-infrared STED nanoscopy with an engineered bacterial phytochrome. *Nat Commun* **9**, 4762.
23. Ye S, Yan W, Zhao M, Peng X, Song J, Qu J (2018) Low-saturation-intensity, high-photostability, and high-resolution STED nanoscopy assisted by $CsPbBr_3$ quantum dots. *Adv Mater* **30**, 1800167.
24. Heilemann M (2010) Fluorescence microscopy beyond the diffraction limit. *J Biotechnol* **149**, 243–251.
25. Zhang C, Yu B, Lin F, Samanta S, Yu H, Zhang W, Jing Y, Shang C, et al (2023) Deep tissue super-resolution imaging with adaptive optical two-photon multifocal structured illumination microscopy. *PhotoniX* **4**, 38.
26. Golovynskyi S, Datsenko OI, Seravalli L, Trevisi G, Frigeri P, Gombia E, Babichuk IS, Lin D, et al (2020) Near-infrared lateral photoresponse in InGaAs/GaAs quantum dots. *Semicond Sci Technol* **35**, 055029.
27. Dong H, Sun LD, Yan CH (2020) Lanthanide-doped upconversion nanoparticles for super-resolution microscopy. *Front Chem* **8**, 619377.
28. Shu Q, Yang L, Zhang X, Yang F, Huang P (2025) Germanium quantum dots prepared by direct annealing of as-deposited amorphous films: Structure and optical properties. *ScienceAsia* **51**, ID 2025036.
29. Hu C, Wu Z, Yang X, Zhao W, Ma C, Chen M, Xi P, Chen H (2020) MUTE-SIM: Multiphoton up-conversion time-encoded structured illumination microscopy. *OSA Contin* **3**, 594.
30. Minoshima M, Kikuchi K (2017) Photostable and photoswitching fluorescent dyes for super-resolution imaging. *J Biol Inorg Chem* **22**, 639–652.
31. Jing Y, Huang L, Dong Z, Gong Z, Yu B, Lin D, Qu J (2024) Super-resolution imaging of folate receptor alpha on cell membranes using peptide-based probes. *Talanta* **268**, 125286.
32. Owen DM, Sauer M, Gaus K (2012) Fluorescence localization microscopy: The transition from concept to biological research tool. *Commun Integr Biol* **5**, 345–349.
33. Willig KI, Steffens H, Gregor C, Herholt A, Rossner MJ, Hell SW (2014) Nanoscopy of filamentous actin in cortical dendrites of a living mouse. *Biophys J* **106**, L01–L03.
34. Subach OM, Patterson GH, Ting LM, Wang Y, Condeelis JS, Verkhusha VV (2011) A photoswitchable orange-to-far-red fluorescent protein, PSmOrange. *Nat Methods* **8**, 771–777.
35. Chu J, Haynes RD, Corbel SY, Li P, González GE, Burg JS, Ataie NJ, Lam AJ, et al (2014) Non-invasive intravital imaging of cellular differentiation with a bright red-excitable fluorescent protein. *Nat Methods* **11**, 572–578.
36. Strack RL, Hein B, Bhattacharyya D, Hell SW, Keenan RJ, Glick BS (2009) A rapidly maturing far-red derivative of DsRed-Express2 for whole-cell labeling. *Biochemistry* **48**, 8279–8281.
37. Hense A, Prunsche B, Gao P, Ishitsuka Y, Nienhaus K, Ulrich Nienhaus G (2015) Monomeric Garnet, a far-red fluorescent protein for live-cell STED imaging. *Sci Rep* **5**, 18006.
38. Morozova KS, Piatkevich KD, Gould TJ, Zhang J, Bewersdorf J, Verkhusha VV (2010) Far-red fluorescent protein excitable with red lasers for flow cytometry and superresolution STED nanoscopy. *Biophys J* **99**, L13–L15.
39. Pennacchietti F, Alvelid J, Morales RA, Damenti M, Ollech D, Oliinyk OS, Shcherbakova DM, Villablanca EJ, et al (2023) Blue-shift photoconversion of near-infrared fluorescent proteins for labeling and tracking in living

cells and organisms. *Nat Commun* **14**, 8402.
40. Shcherbakova DM, Baloban M, Emelyanov AV, Brenowitz M, Guo P, Verkhusha VV (2016) Bright monomeric near-infrared fluorescent proteins as tags and biosensors for multiscale imaging. *Nat Commun* **7**, 12405.
41. Wegner W, Ilgen P, Gregor C, Dort JV, Mott AC, Steffens H, Willig KI (2017) *In vivo* mouse and live cell STED microscopy of neuronal actin plasticity using far-red emitting fluorescent proteins. *Sci Rep* **7**, 11781.
42. Li L, Yang Y, Zhang J, Wang X, Ye Z (2025) FOXP3 influences recruitment and polarization of macrophages via regulating CCL5 in non-small cell lung cancer. *ScienceAsia* **51**, ID 2025021.
43. Zhong X, Wang X, Li J, Hu J, Cheng L, Yang X (2021) Ros-based dynamic therapy synergy with modulating tumor cell-microenvironment mediated by inorganic nanomedicine. *Coord Chem Rev* **437**, 213828.
44. Liu Y, Kong D, Song J, Wang Z, Guo Y, Yu L, Gao X, Pak YL, et al (2025) Anionic heptamethine cyanine as reactive sulfur species-activated probe: Application of NIR-II fluorescence imaging for *in vivo* visualization of glutathione. *Sens Actuators B Chem* **430**, 137371.
45. Supabowornsathit K, Faikhruea K, Vilaivan T (2025) Styryl-cyanine dyes: State of the art and applications in bioimaging. *ScienceAsia* **51S**, ID 2025s008.
46. Wu Z, Zhang C, Sha J, Jing Z, He J, Bai Y, Wu J, Zhang S, et al (2024) Ultrabright xanthene fluorescence probe for mitochondrial super-resolution imaging. *Anal Chem* **96**, 5134–5142.
47. Li X, Fan M, Wang Z, Li D, Wu S, Cui X, Xiao Y, Zhang X (2024) Bodipy-based NIR trackers with acidity-driven amphiphilicity for STED super-resolution imaging of lysosomal membranes. *Anal Chem* **96**, 2958–2967.
48. Collot M, Ashokkumar P, Anton H, Boutant E, Faklaris O, Galli T, Mely Y, Danglot L, et al (2019) Membright: A family of fluorescent membrane probes for advanced cellular imaging and neuroscience. *Cell Chem Biol* **26**, 1–15.
49. Salam A, Kaushik K, Mukherjee B, Anjum F, Sapkal GT, Sharma S, Garg R, Nandi CK (2024) A zinc metal complex as an NIR emissive probe for real-time dynamics and *in vivo* embryogenic evolution of lysosomes using super-resolution microscopy. *Chem Sci* **15**, 15659–15669.
50. Ha T, Tinnefeld P (2012) Photophysics of fluorescent probes for single-molecule biophysics and super-resolution imaging. *Annu Rev Phys Chem* **63**, 595–617.
51. Ye Z, Yu H, Yang W, Zheng Y, Li N, Bian H, Wang Z, Liu Q, et al (2019) Strategy to lengthen the on-time of photochromic rhodamine spirolactam for super-resolution photoactivated localization microscopy. *J Am Chem Soc* **141**, 6527–6536.
52. Takakura H, Zhang Y, Erdmann RS, Thompson AD, Lin Y, McNellis B, Rivera-Molina F, Uno SN, et al (2017) Long time-lapse nanoscopy with spontaneously blinking membrane probes. *Nat Biotechnol* **35**, 773–780.
53. Tyson J, Hu K, Zheng S, Kidd P, Dadina N, Chu L, Toomre D, Bewersdorf J, et al (2021) Extremely bright, near-IR emitting spontaneously blinking fluorophores enable ratiometric multicolor nanoscopy in live cells. *ACS Cent Sci* **7**, 1419–1426.
54. Wu ZH, Zhu X, Yang Q, Zagranyarski Y, Mishra K, Strickfaden H, Wong RP, Basché T, et al (2024) Near-infrared perylenecarboximide fluorophores for live-cell super-resolution imaging. *J Am Chem Soc* **146**, 7135–7139.
55. Masch JM, Steffens H, Fischer J, Engelhardt J, Hubrich J, Keller-Findeisen J, D'Este E, Urban NT, et al (2018) Robust nanoscopy of a synaptic protein in living mice by organic-fluorophore labeling. *Proc Natl Acad Sci USA* **115**, E8047–E8056.
56. Virant D, Traenkle B, Maier J, Kaiser PD, Bodenhofer M, Schmees C, Vojnovic I, Pisak-Lukats B, et al (2018) A peptide tag-specific nanobody enables high-quality labeling for dSTORM imaging. *Nat Commun* **9**, 930.
57. Yang Q, Failla AV, Turunen P, Mateos-Maroto A, Gai M, Zuschratter W, Westendorf S, Gelléri M, et al (2025) Reactivatable stimulated emission depletion microscopy using fluorescence-recoverable nanographene. *Nat Commun* **16**, 1341.
58. Yin J, Zhang J, Chen M, Yin H, Tian J (2022) Reduction of Cd^{2+}/Ag^{+}-induced toxicity by 3-mercaptopropionic acid-CdSe/ZnS quantum dots and glutathione-CdSe/ZnS quantum dots in human liver cancer cells. *ScienceAsia* **48**, 414–422.
59. Sun Z, Liu Z, Chen H, Li R, Sun Y, Chen D, Xu G, Liu L, et al (2019) Semiconducting polymer dots with modulated photoblinking for high-order super-resolution optical fluctuation imaging. *Adv Optical Mater* **7**, 1900007.
60. Chaisrisongkram C, Thiwawong T, Onlaor K, Tunhoo B (2024) Preparation of calcium oxide/graphitic carbon nitrides ($CaO/g\text{-}C_3N_4$) composite for photocatalyst dye degradation. *ScienceAsia* **50**, ID 2024066.
61. Chen C, Wang F, Wen S, Su QP, Wu MCL, Liu Y, Wang B, Li D, et al (2018) Multi-photon near-infrared emission saturation nanoscopy using upconversion nanoparticles. *Nat Commun* **9**, 3290.
62. Liu B, Chen C, Di X, Liao J, Wen S, Su QP, Shan X, Xu ZQ, et al (2020) Upconversion nonlinear structured illumination microscopy. *Nano Lett* **20**, 4775–4781.
63. Hanne J, Falk HJ, Görlitz F, Hoyer P, Engelhardt J, Sahl SJ, Hell SW (2015) STED nanoscopy with fluorescent quantum dots. *Nat Commun* **6**, 7127.
64. Fang H, Yao S, Chen Q, Liu C, Cai Y, Geng S, Bai Y, Tian Z, et al (2019) *De novo*-designed near-infrared nanoaggregates for super-resolution monitoring of lysosomes in cells, in whole organoids, and *in vivo*. *ACS Nano* **13**, 14426–14436.
65. Xu R, Dang D, Wang Z, Zhou Y, Xu Y, Zhao Y, Wang X, Yang Z, et al (2022) Facilely prepared aggregation-induced emission (AIE) nanocrystals with deep-red emission for super-resolution imaging. *Chem Sci* **13**, 1270–1280.
66. Zhou L, Cao H, Huang L, Jing Y, Wang M, Lin D, Yu B, Qu J (2023) Narrowband photoblinking InP/ZnSe/ZnS quantum dots for super-resolution multifocal structured illumination microscopy enhanced by optical fluctuation. *Nanophotonics* **12**, 1777–1785.
67. Zhou L, Yu B, Huang L, Cao H, Lin D, Jing Y, Wali F, Qu J (2022) Nonblinking core-multishell InP/ZnSe/ZnS quantum dot bioconjugates for super-resolution imaging. *ACS Appl Nano Mater* **5**, 18742–18752.
68. Golovynskyi S, Datsenko OI, Seravalli L, Trevisi G, Frigeri P, Li B, Lin D, Qu J (2021) InAs/InGaAs quantum dots confined by inalas barriers for enhanced room temperature light emission: Photoelectric properties and

deep levels. *Microelectron Eng* **238**, 11514.
69. Jing Y, Liu G, Zhang C, Yu B, Sun J, Lin D, Qu J (2022) Lipophilic red-emitting carbon dots for detecting and tracking lipid droplets in live cells. *ACS Appl Bio Mater* **5**, 1187–1193.
70. Liu Z, Li J, Zhao C, Zhang Z, Wu P, Chen J, He X, Zhang S, et al (2025) Molecular engineering enables bright carbon dots for super-resolution fluorescence imaging and *in vivo* optogenetics. *Adv Mater* **37**, 2410786.
71. Liu X, Chen SY, Chen Q, Yao X, Gelléri M, Ritz S, Kumar S, Cremer C, et al (2019) Nanographenes: Ultrastable, switchable, and bright probes for super-resolution microscopy. *Angew Chem Int Ed* **59**, 496–502.
72. Guo J, Fan J, Liu X, Zhao Z, Tang BZ (2020) Photomechanical luminescence from through-space conjugated AIEgens. *Angew Chem Int Ed* **59**, 8828–8832.
73. Godin AG, Setaro A, Gandil M, Haag R, Adeli M, Reich S, Cognet L (2019) Photoswitchable single-walled carbon nanotubes for super-resolution microscopy in the near-infrared. *Sci Adv* **5**, eaax1166.
74. Chang Y, Kim DH, Zhou K, Jeong MG, Park S, Kwon Y, Hong TM, Noh J, et al (2021) Improved resolution in single-molecule localization microscopy using QD-PAINT. *Exp Mol Med* **53**, 384–392.
75. Dolai J, Joshi P, Mondal PP, Maity A, Mukherjee B, Jana NR (2024) Blinking carbon dots as a super-resolution imaging probe. *ACS Appl Mater Interfaces* **16**, 16003–16010.
76. Sun X, Mosleh N (2023) Fluorescent carbon dots for super-resolution microscopy. *Materials* **16**, 890.
77. Li W, Kaminski Schierle GS, Lei B, Liu Y, Kaminski CF (2022) Fluorescent nanoparticles for super-resolution imaging. *Chem Rev* **122**, 12495–12543.